Electronic Supplementary Material (ESI) for Journal of Materials Chemistry A.
This journal is © The Royal Society of Chemistry 2020

Supporting Information

Bimetallenes for Selective Electrocatalytic Conversion of CO_2: A First-Principles Study

Zhonglong Zhao[a] *and Gang Lu**[b]

[a.] School of Physical Science and Technology, Inner Mongolia University, Hohhot 010021, China

[b.] Department of Physics and Astronomy, California State University Northridge, California 91330, United States

AUTHOR INFORMATION

Corresponding Author

*Email: ganglu@csun.edu

Computational details

1. Free energy calculations

The reaction free energy of the intermediates is derived from the binding energy (E_B) at 18.5 °C by including the zero-point energy (ZPE), heat capacity (C_P) and entropy (-TS) corrections:[1]

$$G = E_B + ZPE + \int C_P dT - TS \quad (1)$$

All the free energy corrections are calculated based on the molecular vibration analysis and assuming that the changes in the vibrations of the surface caused by the intermediate are minimal. We applied approximate solvation corrections to the reaction intermediates proposed by Peterson et al.[2] since an explicit treatment of the salvation is computationally highly expensive. The binding energy of an intermediate is calculated as:

$$E_B[C_xH_yO_z] = E[C_xH_yO_z] - E_{slab} - xE_C - yE_H - zE_O \quad (2)$$

Where $E[C_xH_yO_z]$ and E_{slab} denote the total energy of the system with and without the intermediate, respectively. E_C, E_H, and E_O are the total energy of one atom in grapheme, gaseous hydrogen, and the difference between H_2O and H_2, respectively.

2. Activation barrier calculations

The activation barrier for the hydrogenation of b-CO_2 is calculated based on the model proposed by Nie et al.[3-4] In the model, the activation barrier for an elementary electrochemical reaction ($A^* + H^+ + e^- \rightarrow AH^*$) can be derived from the analogous surface hydrogenation reaction ($A^* + H^* \rightarrow AH^*$). The model is rationalized by the assumption that the former is an inner-sphere reaction and the transition state is reached when the proton arrives at the adsorbed species, A*. The electron transfer is considered ultrafast once the proton attains the transition state. The activation barrier as a function of the electrode potential U is calculated as:

$$E_{act}(U) = E_{act}^0 + \beta'(U - U^0) \quad (3)$$

where E_{act}^0 is the reaction barrier calculated from DFT plus the ZPE correction. U^0 is set so that the chemical potential of the adsorbed H* is equal to that of a proton-electron pair. β' is an effective symmetry factor calculated by:

$$\beta' = 0.5 + (\mu_{TS} - \mu_{reactant})/3 \quad (4)$$

where $\mu_{TS} - \mu_{reactant}$ represents the variation in the surface dipole moments between the reactant and the transition state.

In the activation barrier calculations, an ice-like water bilayer (H-down configuration)[5] was added above the adsorbed reactants to simulate the solvation effect. Besides, one more water molecule was added on the surface to assist the hydrogenation reactions.[6] More specifically, water can assist the reaction in two different manners, which are referred to as the water-solvated (WS) model and H-shuttling (HS) model. In the WS model, the surface proton is transferred directly to the b-CO_2 (to form COOH* or HCOO*), assisted by the hydrogen bond between the water molecule and b-CO_2. In the HS model, however, the surface proton is transferred to the water molecule, which concurrently shuttles another proton to b-CO_2, analogous to the Grotthuss mechanism. We find that the reaction barriers for the reduction of b-CO_2 can be lowered in the water-assisted reaction models compared with the hydrogenation without the assistance of water. Besides, the WS model is more favored for the reduction of b-CO_2 into HCOO*, by which the surface proton is transferred to the C atom of b-CO_2. The HS model is more favored for the reduction of b-CO_2 into COOH*, by which the proton is shuttled by water to one of the O atoms of b-CO_2.

References

(1) Cramer, C. J. *Essentials of computational chemistry: theories and models*. 2nd ed.; Wiley & Sons: Chichester, U.K., 2004.

(2) Peterson, A. A.; Abild-Pedersen, F.; Studt, F.; Rossmeisl, J.; Norskov, J. K. How copper catalyzes the electroreduction of carbon dioxide into hydrocarbon fuels. *Energy Environ. Sci.* **2010,** *3*, 1311-1315.

(3) Nie, X.; Esopi, M. R.; Janik, M. J.; Asthagiri, A. Selectivity of CO_2 reduction on copper electrodes: the role of the kinetics of elementary steps. *Angew. Chem., Int. Ed.* **2013,** *52*, 2459-2462

(4) Nie, X.; Luo, W.; Janik, M. J.; Asthagiri, A. Reaction mechanisms of CO_2 electrochemical reduction on Cu (111) determined with density functional theory. *J. Catal.* **2014,** *312*, 108-122.

(5) Ogasawara, H.; Brena, B.; Nordlund, D.; Nyberg, M.; Pelmenschikov, A.; Pettersson, L. G. M.; Nilsson, A. Structure and bonding of water on Pt (111). *Phys. Rev. Lett.* **2002**, *89*, 276102.

(6) Zhao, Z.; Lu, G. Cu-based single-atom catalysts boost electroreduction of CO_2 into CH_3OH: first-principles predictions. *J. Phys. Chem. C* **2019**, *123*, 4380-4387.

Table S1. Segregation energies of the studied bimetallenes. Row and column indicate solute and host metals, respectively. All values are in eV. Positive value indicates that the bimetallene is stable.

	Ti	V	Cr	Mn	Fe	Co	Ni	Cu	Zn
Ag	0.547	0.538	0.507	0.273	0.229	0.238	0.303	0.091	-0.130
Au	0.639	0.592	0.586	0.436	0.359	0.384	0.445	0.331	0.119
Cu	0.315	0.511	0.049	0.074	0.236	0.323	0.230	0.000	-0.292
Pd	0.867	0.751	0.529	0.444	0.556	0.312	0.231	0.143	0.111
Pt	1.335	1.206	0.978	0.820	0.960	0.853	0.678	0.544	0.515

	Zr	Nb	Mo	Ru	Rh	Pd	Ag	Cd
Ag	0.616	0.679	0.571	0.427	0.338	0.224	0.000	-0.281
Au	0.592	0.619	0.536	0.340	0.330	0.300	0.149	-0.101
Cu	0.003	0.371	0.449	0.154	0.001	-0.114	-0.536	-0.924
Pd	0.936	1.107	1.003	0.542	0.272	0.000	-0.267	-0.271
Pt	1.244	1.419	1.256	0.733	0.402	0.081	-0.204	-0.247

	Hf	Ta	W	Re	Os	Ir	Pt	Au
Ag	0.602	0.689	0.611	0.572	0.464	0.340	0.201	-0.110
Au	0.578	0.563	0.471	0.476	0.263	0.240	0.215	0.000
Cu	0.177	0.480	0.550	0.513	0.213	-0.007	-0.156	-0.621
Pd	1.014	1.118	1.059	1.032	0.667	0.393	0.035	-0.392
Pt	1.397	1.520	1.374	1.149	0.791	0.421	0.000	-0.442

Table S2. Free energy changes for the initial reduction of CO_2 into COOH* and HCOO* on the proposed bimetallenes.

bimetallenes	ΔG ($CO_2 \rightarrow$ COOH*), eV	ΔG ($CO_2 \rightarrow$ HCOO*), eV
CuCo	0.820	0.235
CuZr	0.780	-0.002
CuHf	0.720	0.076
AgTi	0.879	0.236
AgV	1.101	0.362
AgCr	1.170	0.497
AgMn	1.137	0.451
AgFe	1.042	0.380
AgCo	1.123	0.445
AgNi	1.135	0.449
AgCu	1.111	0.474
AgZr	0.863	0.258
AgNb	0.742	0.135
AgRu	0.947	0.352
AgPd	1.152	0.497
AgHf	0.854	0.243
AgTa	0.700	0.062
AgW	0.831	0.209
AgRe	0.901	0.311
AgOs	0.893	0.305
AgPt	1.073	0.405

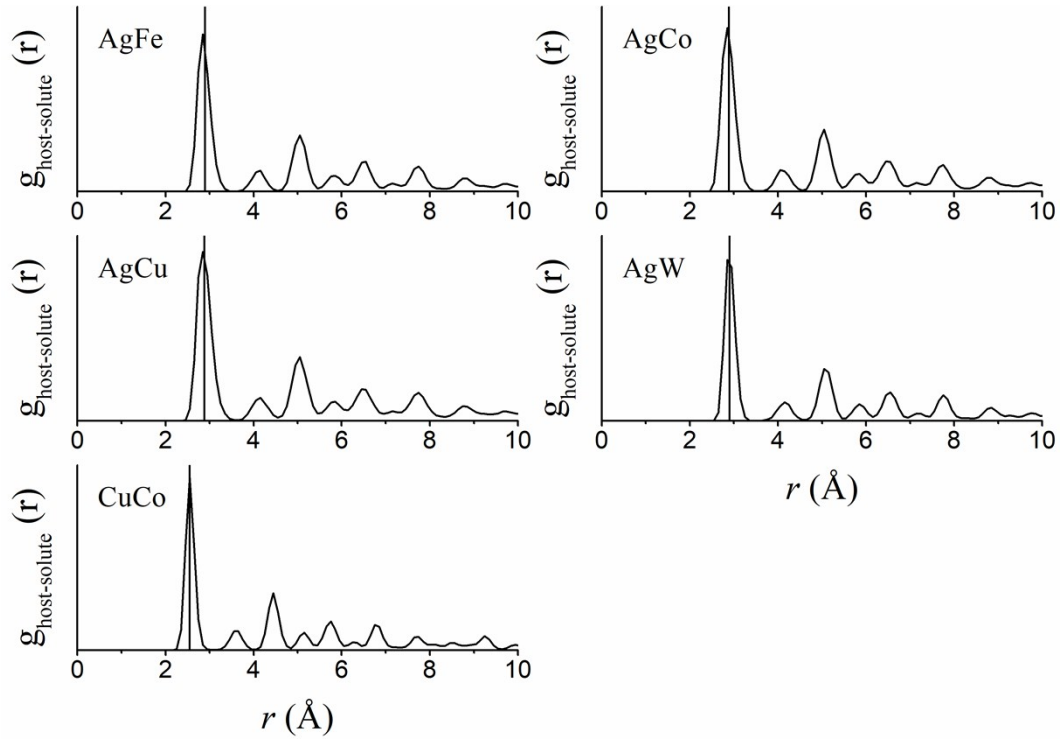

Figure S1. Radial distribution function of the selected bimetallenes at 300 K in the presence of HCOO* on the surface. The vertical lines indicate the equilibrium nearest-neighbor distance at 0 K, which is essentially the same at 300 K after a 4 ps MD simulation.

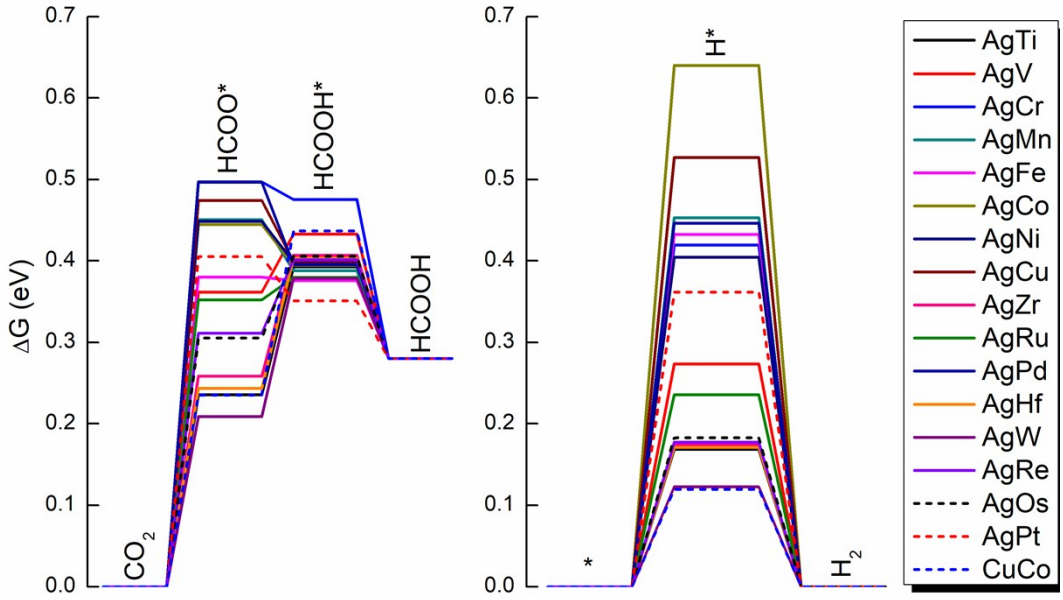

Figure S2. Free energy diagrams toward HCOOH production (left) and HER (right) on the 17 proposed bimetallenes.